Semiconductor-Assisted Self-Cleaning Polymeric Fibers Based on Zinc Oxide Nanoparticles

Hadi Fallah Moafi, Abdollah Fallah Shojaie, Mohammad Ali Zanjanchi

Department of Chemistry, Faculty of Science, University of Guilan, Rasht, Iran

Received 29 June 2010; accepted 14 January 2011
DOI 10.1002/app.34179
Published online 12 April 2011 in Wiley Online Library (wileyonlinelibrary.com).

ABSTRACT: Self-cleaning polymeric fibers have been successfully prepared by depositing ZnO nanoparticle onto wool and polyacrylonitrile (PAN) fibers with good compatibility and significant photocatalytic self-cleaning activity using the sol-gel process at ambient temperature. scanning electron microscopy, energy dispersive spectroscopy, transmission electron microscopy, diffuse reflectance spectroscopy, X-ray diffraction, Brunauer-Emmett-Teller surface area analysis, and thermogravimetric analysis have been adopted as the characterization techniques. Transmission electron microscopy studies revealed presence of zinc oxide nanoparticles with 10–15 nm in size. Brunauer-Emmett-Teller measurement showed surface area of 48 m^2/g for the ZnO nanoparticles. Photocatalytic activity of the self-cleaning materials were tested by measuring the photo-assisted degradation of methylene blue (MB) and eosin yellowish (EY) under ultraviolet-visible illumination. The results indicate that both of the ZnO-coated polyacrylonitrile and ZnO-coated wool fibers acquire photocatalytic activity toward dyes degradation. The photocatalytic activity of the treated fibers is maintained upon several numbers of photodegradation cycles. This facile and cheap preparation technique can be also applied to new polymeric fabrics to produce self-cleaning materials for industrial application. © 2011 Wiley Periodicals, Inc. J Appl Polym Sci 121: 3641–3650, 2011

Key words: zinc oxide nanoparticles; photocatalytic activity; polyacrylonitrile; sol-gel; self-cleaning materials; wool

INTRODUCTION

Recently, it has been demonstrated that semiconducting materials capable of mediating photocatalytic oxidation of organic compounds, can be an alternative to the conventional methods for the removal of resistant organic pollutants from environment.[1] Among the oxide semiconductors used, ZnO and TiO_2 are the most extensively used photocatalysts due to their high photocatalytic activity, nontoxic nature, inexpensive cost, excellent chemical, and mechanical stability. Although TiO_2 is universally considered as the most active photocatalyst, ZnO can also be a suitable alternative to TiO_2 because it is lower in cost and has the similar band gap energy around 3.2 eV. In addition, ZnO shows better performance compared with TiO_2 in the degradation of several organic contaminants in both acidic and basic media, which has stimulated many researchers for further exploration of the properties of ZnO in many photocatalytic reactions.[1–6]

One of the most important applications of photocatalytic oxidation processes is the development of self-cleaning materials. Recently, self-cleaning materials coated with photocatalytic TiO_2 film have been attractive for many researchers.[7–14] Their capability of self-cleaning mainly depends on the photocatalytic activity and amphipathic properties (hydrophilicity and hydrophobicity) of nanosized semiconductor films.[15] The irradiation of the nano-oxide semiconductors on the surface of self-cleaning materials can decompose toxic pollutants by highly active species (like O_2^-,$^\bullet$OH, $^\bullet$OOH) produced from the reaction between photogenerated electrons (or holes) and oxygen (water). The properties of self-cleaning materials mentioned above lead to promising applications in automobile windshields, windows of high-rise buildings, and other fields utilized for sterilization, deodorization, antifog, self-cleaning, and room air cleaning.[7]

ZnO is known to be one of the important photocatalyst because of its many advantages, such as low price, large initial rates of activities, many active sites with high surface reactivity, high absorption efficacy of light radiations, and environmental-safety.[16]

ZnO coating have been prepared by a variety of techniques such as pulsed laser deposition,[17] magnetron sputtering,[18,19] chemical vapor deposition,[20] and sol-gel processing.[21–24] The sol-gel techniques are widely used for ZnO thin films fabrication due to several advantages in comparison with the dry methods deposition. The most important advantages

Correspondence to: A. F. Shojaie (a.f.shojaie@guilan.ac.ir).

are the simple equipment, the ability of accurate control of stoichiometry over large area, high homogeneity and relatively low process temperature.[24]

ZnO coating have been synthesized on some polymeric fibers such as cotton and polyacrylonitrile (PAN) fibers.[25–28] Although, some features such as UV protection,[25] antibacterial properties,[26] superhydrophobicity,[27] and physical properties[28] have been explored, but solid phase photocatalytic self-cleaning has not been carried out so far.

In this work, we report the route that we developed as a facile and effective method to create self-cleaning ZnO coatings on PAN and wool substrates at ambient temperature. In our previous work we compared the photoactivity of TiO_2 and ZrO_2-coated PAN fibers for self-cleaning purpose.[29] The initial precursors for the synthesis of TiO_2 and ZrO_2 onto polymeric surface are relatively expensive. So, in this study, we selected a cheap precursor such as zinc acetate for synthesis of ZnO photocatalyst on PAN and wool fibers. These polymeric fibers with nano ZnO self-cleaning coating exhibited interesting photodegradation properties when exposed to UV-vis illumination.

EXPERIMENTAL

Reagents and materials

Merino wool fibers, characterized by 35 μm diameter and PAN fiber (20 μm diameter), were used in the entire processes. PAN fiber was provided by Daqing PAN Corp., PR China. The PAN used was a copolymer of 90% acrylonitrile and 10% methylacrylate. Zinc acetate dehydrate, methanol, sodium hydroxide, methylene blue (MB), and eosin yellowish (EY) were obtained from Merck (Germany).

Synthesis procedure

The typical procedure for the synthesis of ZnO-sol is based on the method described in the literature with minor changes in details.[30] Zinc acetate dihydrate was used as zinc oxide source. In a typical procedure 0.01 mol of zinc acetate dihydrate were dissolved in 50 mL of methanol and heated at 50°C along with vigorous stirring for half an hour, thus making precursor solution A. Then 0.02 mol of sodium hydroxide were dissolved in 50 mL of methanol and heated at 50°C along with vigorous stirring for 1 h, making precursor solution B. To make ZnO nano-sol, solution B was added into the solution A drop wise under constant stirring for half an hour and then the mixture were heated at 50°C for another half an hour. Subsequently, after continuous stirring for 2 h and cooling at room temperature, a homogenous and transparent solution was obtained.

For the impregnation, the polymeric fibers were washed first by water and detergent at 50°C for 30 min to remove the impurities such as wax, fat, etc., and then washed several times by a large amount of deionized water. They were further cleaned in acetone for 60 min and dried at room temperature for 24 h. The fibers dried in a preheated oven and then immersed in the ZnO sol for 5 min. The samples were then placed in 70°C preheated oven to remove the solvent from the fibers and then heated at 150°C for 30 min, to complete the formation of zinc oxide. Finally, the impregnated fibers were rinsed in distilled water for about 10 min shaking by hand. During this step the unattached ZnO particles were removed from the fibers surface.

Photocatalytic test

The photocatalytic activities of the nano zinc oxide coated fibers have been investigated by exposing the samples containing preadsorbed MB and EY to UV-vis light. For this purpose, 100 mL aqueous solutions (1.0×10^{-5} mol/L) of MB and EY were prepared separately. Both bare and coated fibers are treated in MB and EY solutions. The same amount of each sample was immersed under mild stirring in the same volume of the solution and remained overnight to complete the adsorption. The fibers were recovered and dried at room temperature. The so-obtained samples (coated-fibers) were cut into 2×2 cm^2 pieces which they have fixed in the front of the integrating sphere hole of the diffuse reflectance attachment. These selected samples were exposed to UV-vis to test their photoactivity. The similar settings were performed in several interval times during the test. For photocatalytic reactions, the irradiation was carried out on the dry samples, by means of a high-pressure mercury lamp (HPMV 400W, Germany). The lamp yields an illumination spectrum ranging from ultraviolet to visible (200–800 nm). Details were described in our previous work.[29]

The photocatalytic decomposition efficiency was determined from the following equation:

$$\text{Photocatalytic decomposition efficiency} = [(C_0 - C)/C_0] \times 100 = [(A_0 - A)/A_0] \times 100$$

where, C_0 represents the initial concentration of the dyes on fiber surface, C the final concentration after illumination by UV light, A_0 the initial absorbance, and A the variable absorbance. The reusability of the ZnO-coated fibers was checked by consecutive repeated adsorption of the dyes and testing the photoactivity of the sample for the new degradation cycle. This procedure was repeated three times on the same sample as described above for both MB and EY solutions.

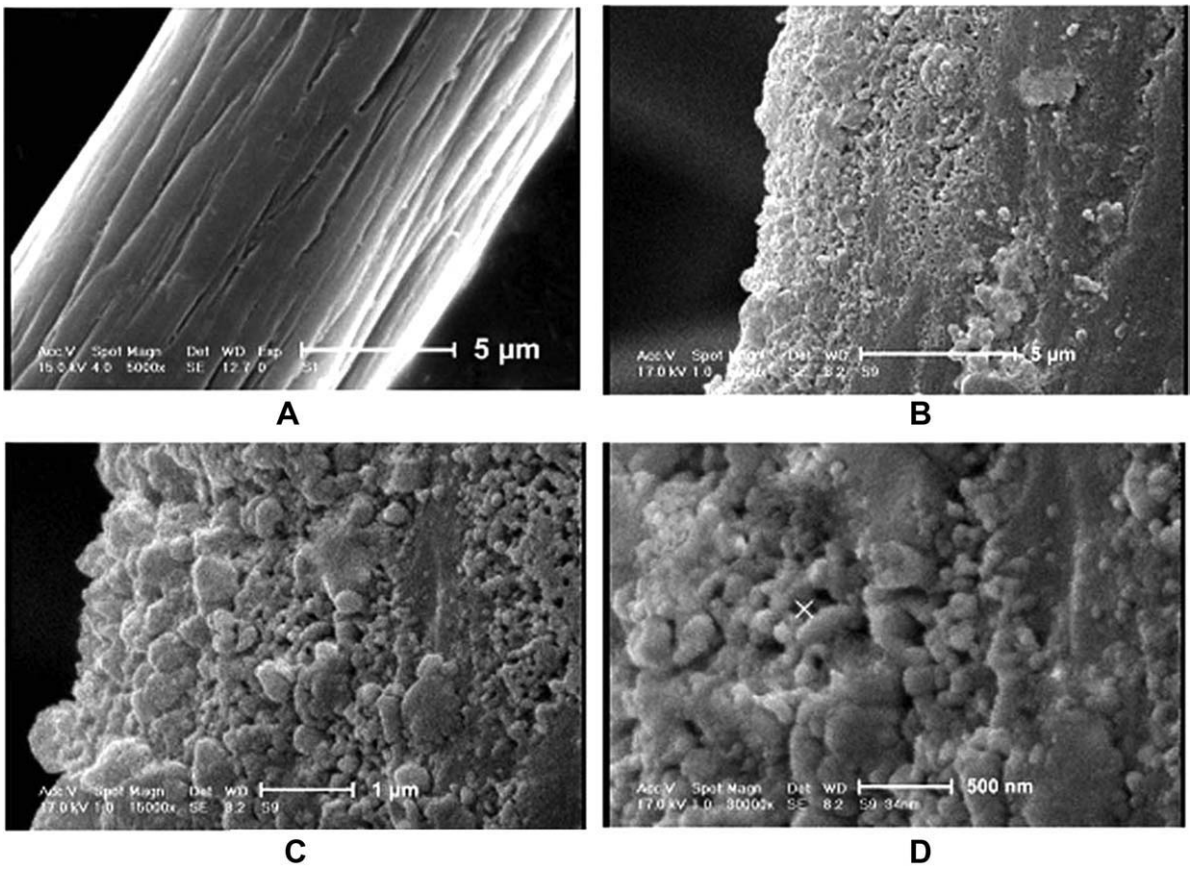

Figure 1 SEM images of: (A) pure PAN fiber (×5000), (B) ZnO-coated fiber (×5000), (C) enlarged TiO_2-coated fiber (×15,000), and (D) enlarged ZnO-coated fiber (×30,000).

Characterization techniques

To investigate the morphology of the pure and ZnO-modified fibers, scanning electron microscopy (SEM) images were obtained by a Philips, XL30 equipment. The energy dispersive spectroscopy (EDS) microanalysis system joined to the above instrument was used for compositional analysis of the ZnO-coated fibers. The ZnO particle sizes were obtained by transmission electron microscopy (TEM) using a Philips CM10 instrument with an accelerating voltage of 100 kV. For photodecomposition reaction, the UV-vis reflectance spectra were recorded at room temperature by a UV-2100 Shimadzu Spectrophotometer in the reflectance mode by investigating the evolution of the absorbance. The Brunauer-Emmett-Teller (BET) specific surface area of the synthesized nanoparticles was determined by nitrogen adsorption at liquid nitrogen temperature on a Sibata SA-1100 surface area analyzer. X-ray diffraction (XRD) measurements were recorded by a D8 Bruker advanced diffractometer with Cu-Kα radiation, scan rate 0.02 2θ/s and within a range of 2θ of 10 to 70 degree at room temperature. Thermogravimetric analysis (TGA) was performed in air flow (ramp of 10°K/min) by TGA V5.1A DuPont 2000.

RESULTS AND DISCUSSION

Morphological and compositional analysis

Surface morphology of the bare fibers, ZnO/fibers and sol-derived ZnO powder are shown in Figures 1 and 2. Figures 1(A) and 2(A) show that the surface of the pristine fibers are smooth and clean. Figures 1(B) and 2(B) show that treated fibers after being washed are covered by continuous and homogeneous dispersed ZnO nanoparticles. SEM images revealed that the deposited zinc oxide consisted of fine particles with a diameter of several tens of nanometer. On the other hand, SEM study of ZnO deposited onto fibers, indicate that the particle size of the deposited zinc oxide on the fibers surface are less than 50 nm and deposited particles are spherical [Figs. 1(D) and 2(C)]. Figure 2(D) shows the micrograph of the sol-derived ZnO nanoparticles. It is clear that morphology of the ZnO particle is similar to that of ZnO nanoparticles synthesized on fibers surface.

EDS analysis were used to determine the surface composition of the coated samples. In Figure 3, EDS analysis of ZnO-covered fibers after washing step is reported. On the basis of this result, it is noteworthy to observe that the deposited material consists of

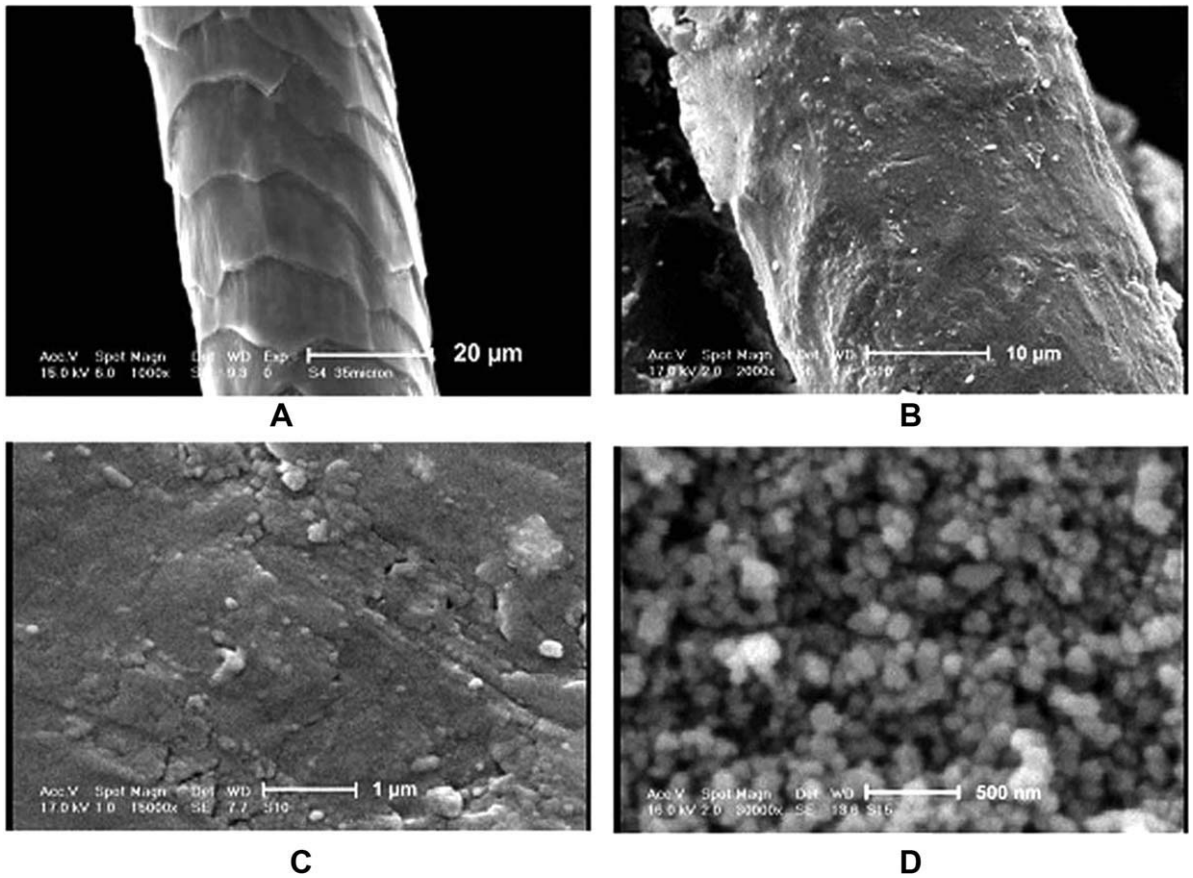

Figure 2 SEM images of: (A) pure wool fiber (×1000), (B) ZnO-coated fiber (×2000), (C) enlarged ZnO-coated fiber (×15,000), and (D) ZnO powder at 150°C (×15,000).

zinc and oxygen, where after washing step, remarkable amount of zinc oxide is still present on the fibers surface. This means that ZnO nanoparticles have sufficient adhesion towards the fibers to resist a washing process.

To investigate the size of ZnO nanoparticles forming on the fibers surface, the particles were analyzed by TEM, as showed in Figure 4. TEM images shows that the deposited zinc oxide consists of uniform spherical particles of average diameter 10–15 nm. The data of the particle sizes are in accord with that of the XRD results. It is noticeable that the spherical ZnO particles are distributed homogenously on the fibers surface.

XRD analysis

The XRD patterns of the pure, ZnO-coated fibers and sol-derived ZnO powders are reported in Figures 5 and 6. Figure 5 (peak a) shows two peaks: the intense one at 17° and the broad one at 29°, which constitute the typical XRD pattern of PAN fibers.[31] In Figure 6 (peak a), the bulk of the X-ray signal originated from the wool substrate. The XRD patterns of coated samples [Figs. 5 (peak b) and 6 (peak b)] indicate that the synthesized ZnO particles on the surfaces are hexagonal wurtzite crystal phase due to the presence of attributive peaks (2θ = 31.68°, 34.34°, 36.13°, 47.38°, 56.49°, 62.71°, and 67.95°) for ZnO-

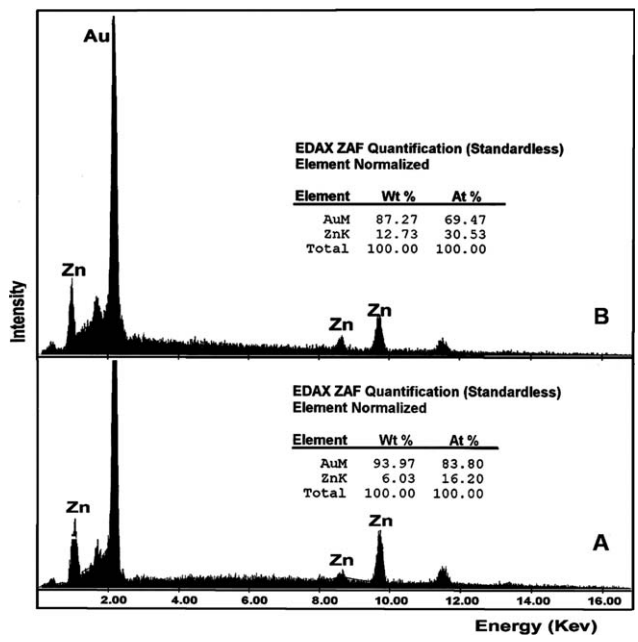

Figure 3 EDS spectra of: (A) ZnO-coated PAN fiber after washing and (B) ZnO-coated wool fiber after washing.

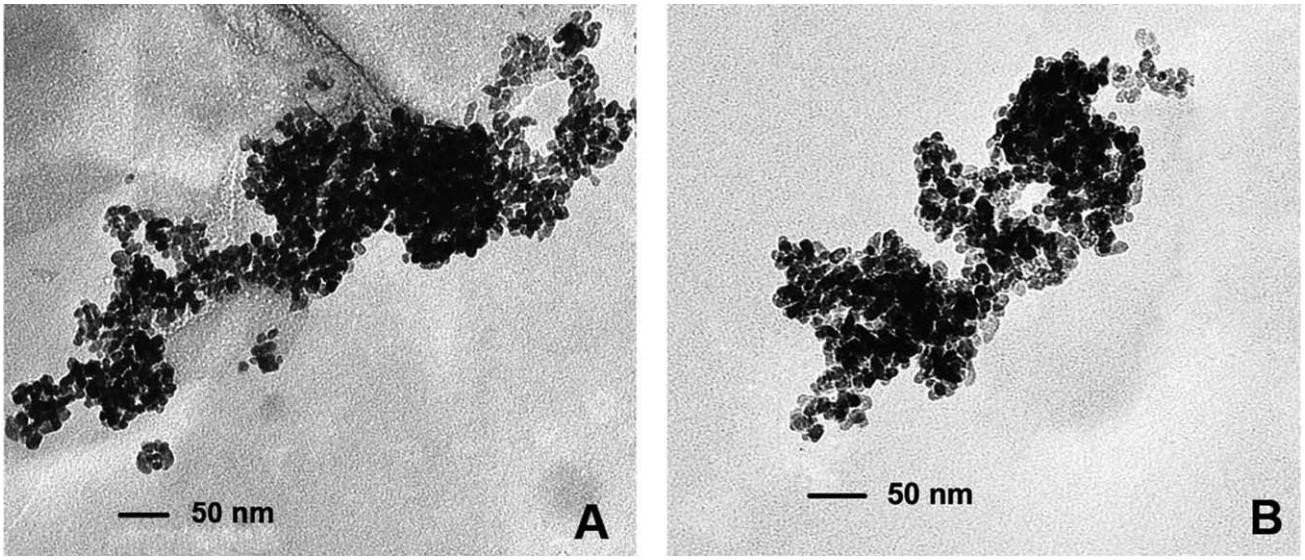

Figure 4 TEM image of: (A) ZnO particles forming on the coated PAN fiber and (B) ZnO particles forming on the coated wool fiber.

coated PAN and $2\theta = 31.56°$, 34.08°, 36.44°, 47.32°, 56.40°, 62.81°, and 67.91° for ZnO-wool fiber. These are associated with diffraction peaks which corresponds to the (100), (002), (101), (102), (110), (103), and (112) planes of the ZnO hexagonal wurtzite structure. Figure 5 (peak c) shows the XRD pattern of sol-derived ZnO powder. It can be seen that all the diffraction peaks could be identified to ZnO peaks with hexagonal wurtzite structure. No other peak related to impurities was detected in the diffractogram which provide further confirmation for the fact that the synthesized powder was single phase of ZnO with hexagonal wurtzite structure.

The crystallite size of nanoparticles can be calculated from Scherrer formula, which can be described as follows:

$$D = \frac{K\lambda}{\beta cos\theta}$$

where D is the grain size, $K = 0.89$, λ the X-ray wavelength (0.15406 nm), θ the Bragg diffraction angle, and β is the peak width at half maximum

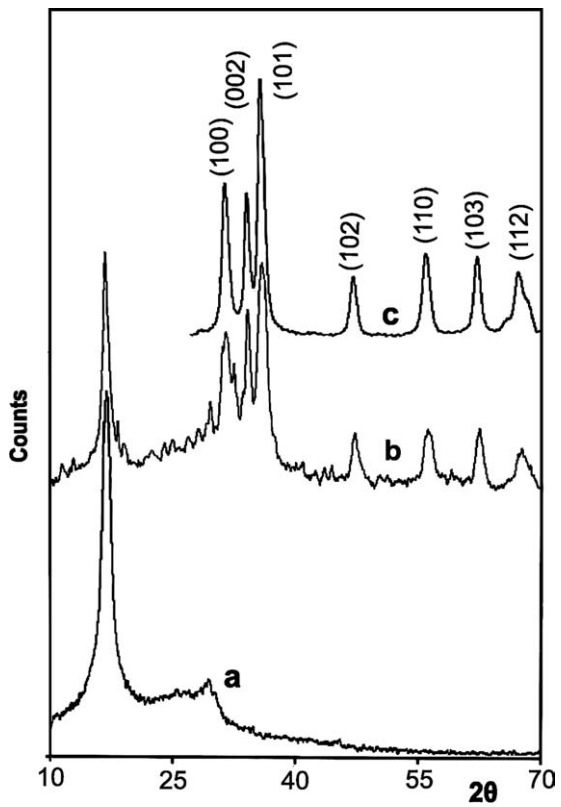

Figure 5 XRD patterns of (a) pure PAN fibers, (b) ZnO-covered fibers at 150°C, and (c) sol-gel-derived ZnO powder at 150°C.

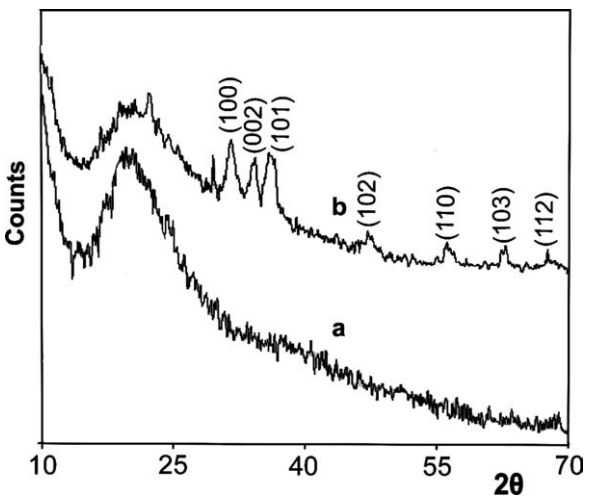

Figure 6 XRD patterns of (a) pure wool fiber and (b) ZnO-covered fibers at 150°C.

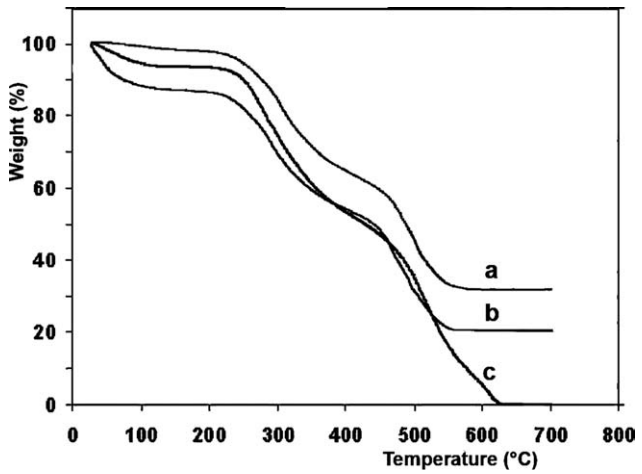

Figure 7 TGA of (a) dried ZnO-coated wool fiber, (b) undried ZnO-coated wool fiber, and (c) pure wool fiber.

(FWHM). The grain sizes of synthesized nano-ZnO onto PAN and wool sample were calculated from the (101) diffraction peak. The grain size of ZnO nanoparticles for ZnO-coated PAN, wool, and sol-derived ZnO powder were 13, 10, and 9 nm, respectively.

Brunauer-Emmett-Teller surface area analysis

In general, the surface area of the catalyst is the most important factor influencing the catalytic activity. The surface area of ZnO particles was determined using the nitrogen gas adsorption method. The surface area of the prepared zinc oxide nanoparticles on glass yielded relatively high surface area (48 m^2/g).

Thermogravimetric analysis

The TGA of the pure and treated fibers was carried out in air atmosphere. Thermograms of the wool and PAN samples are shown in Figures 7 and 8. In Figure 7 (peak c), three main decomposition temperatures were obtained for the pure wool fiber. The initial weight loss at 30–120°C is due to moisture loss. The second and third weight losses took place in the temperature range from 250 to 450°C and 450 to 630°C, respectively. The ZnO-coated samples show similar decomposition stage. For the dried ZnO-coated wool fiber [Fig. 7 (peak a)] the initial weight loss is small. However, for the undried ZnO-coated fiber [Fig. 7 (peak b)] the weight loss is much higher.

The TGA analysis of the pure PAN fiber [Fig. 8 (peak c)] can be roughly divided into three steps according to the extent of weight losses. The first step is up to about 300°C, where weight loss is very small. It is inferred that there is only cyclization occur in this step. The second step is up to about 300°C. During this step, the rate of weight loss becomes quite rapid, which is mainly due to the dehydrogenation. In the last step, fragmentation of polymer chains occur producing volatile species leading to weight loss. The ZnO-coated samples show similar decomposition steps. For the undried ZnO-coated PAN fiber [Fig. 8 (peak b)] more weight loss than pure and dried sample is observed which is due to the adsorbed moisture.

After combustion of all organic parts in the ZnO-modified fibers, the residual amount corresponds to ZnO nanoparticles. From this point, it is indicated that the ZnO nanoparticles were incorporated onto the fibers.

Photocatalytic self-cleaning activity

The photocatalytic activities of the prepared ZnO/ fibers were studied by the degradation experiments using MB and EY dyes as a model compounds. These dyes have strong adsorption characteristics on many surfaces, good resistance to light degradation and a well defined optical absorption maximum in the visible region. There are several methods for evaluating the photocatalytic activity of self-cleaning materials.[7] Three of the mostly used methods are the dye method,[32,33] the stearic acid method,[34,35] and the contact angle method.[36] Recently, Guan et al.[7] have reported a method using the 7-hydroxycoumarin probe, to evaluate the photocatalytic activity of self-cleaning materials. This method is based on monitoring of a highly fluorescent product generated by the self-cleaning materials following UV illumination. In the dye method, the whole process of the photodegradation of dyes under UV irradiation is monitored, and the performance of self-cleaning materials is evaluated with the aid of the decolorization of dyes.

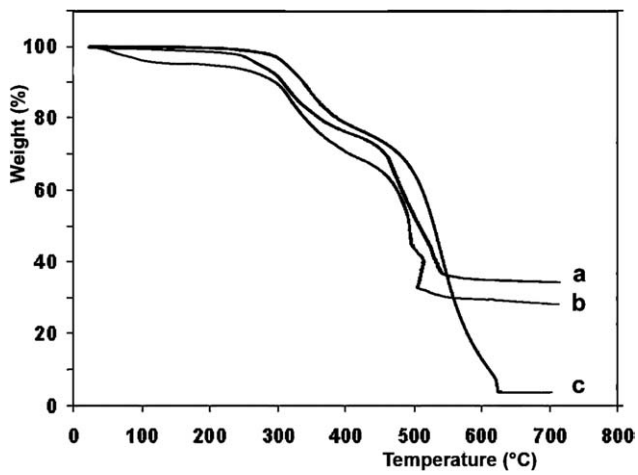

Figure 8 TGA of (a) dried ZnO-coated PAN fiber, (b) undried ZnO-coated PAN fiber, and (c) pure PAN fiber.

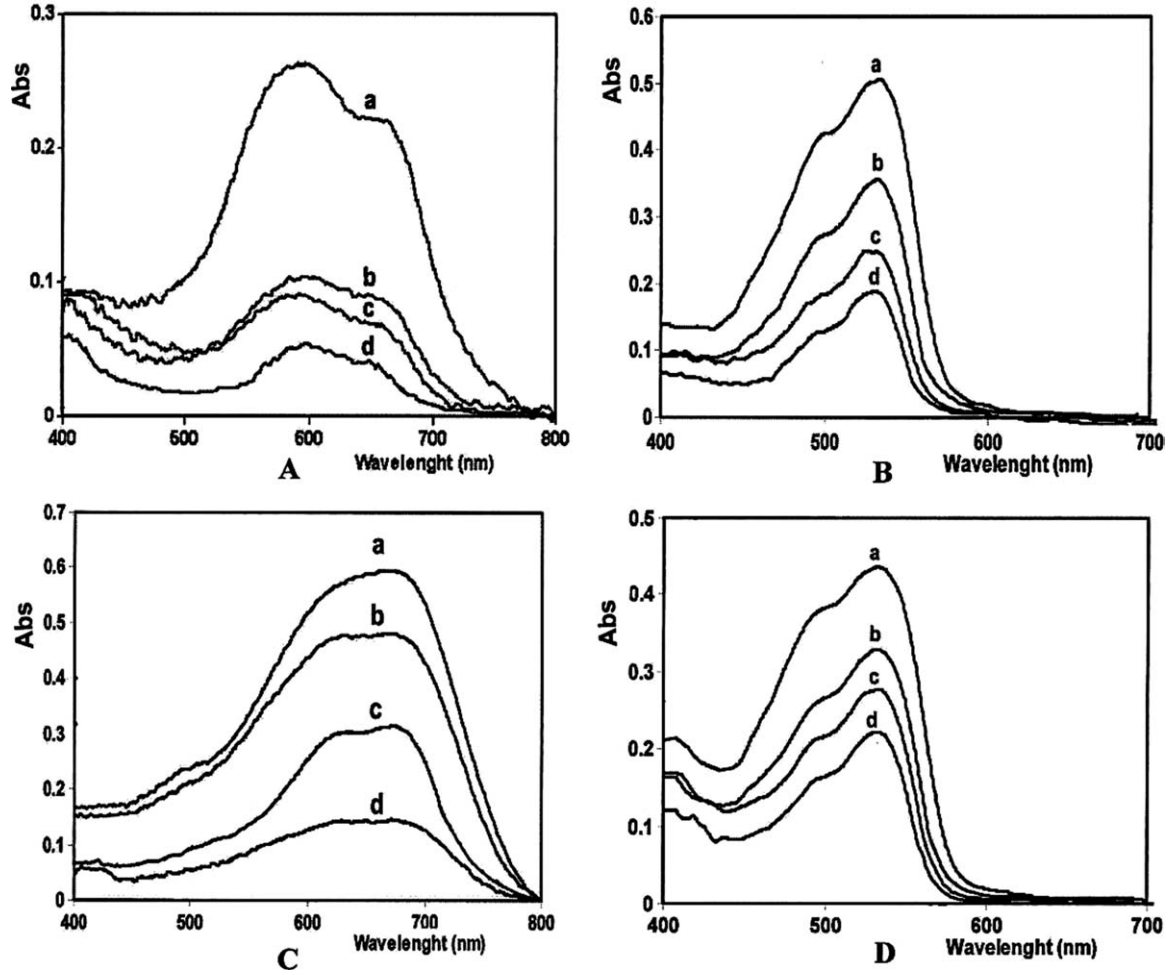

Figure 9 UV-vis reflectance spectra of dyes under UV-vis light irradiation at room temperature: (A) MB on ZnO-coated PAN fiber, (B) EY on ZnO-coated PAN fiber, (C) MB on ZnO-coated wool fiber, and (D) EY on ZnO-coated wool fiber. (a) no exposure, (b) irradiation for 2 h, (c) 4 h, and (d) 6 h.

The photocatalytic activity of our synthesized ZnO on fibers has been investigated by exposing the samples containing preadsorbed MB and EY to UV-vis light. All ZnO-coated samples possessed the ability to decompose dyes upon UV-vis irradiation. The UV-vis reflectance spectra obtained on the coated samples with dyes before (spectrum a) and after illumination (spectrum b–d) are reported in Figure 9. The absorption peaks, corresponding to dye, diminished under reaction which indicates degradation of the dye. No new absorption bands appear in the visible regions. Figure 9(A,C) show that the absorption bands in the 500–700 nm which are due to adsorption of MB, change rapidly because of the catalytic photodegradation (spectrum b–d). This is not unexpected since the photocatalytic activity of ZnO is well known.[37] The disappearance rate of the band due to MB adsorbed on the ZnO-covered fibers is much higher than that observed in case of untreated fibers [Fig. 10 (peaks a, d, e, h)]. It can be seen from Figure 10 (peaks d, h) that in the presence of ZnO and light, 80 and 77% of MB dye were degraded (following an irradiation time of 6 h) upon ZnO-coated PAN and ZnO-coated wool fibers, respectively. This was contrasted with 19 and 22% degradation for the same experiment performed in the absence of ZnO for preadsorbed MB onto pristine PNA and wool fibers [Fig. 10 (peaks a, e)]. These experiments demonstrate that both UV-vis light and ZnO are needed for the effective decomposition of the dye. Similar results have been obtained for the adsorbed EY [Fig. 9(B,D)]. As a matter of fact the adsorption of dye (in the region at 450–600 nm) decreases rapidly under the exposure to UV-vis light. The degradation rate of preadsorbed EY on the ZnO-covered fibers is much higher than that observed in case of untreated fibers [Fig. 10 (peaks b, c, f, g)]. In the presence of both ZnO and UV-vis light illumination 64 and 50% EY dye was degraded for 6 h irradiation time [Fig. 10 (peaks c, g)]. In the absence of ZnO, the degradation efficiency for the preadsorbed EY onto pure PNA and pure wool fibers in the same condition are 37% and 28% [Fig. 10 (peaks b, f)].

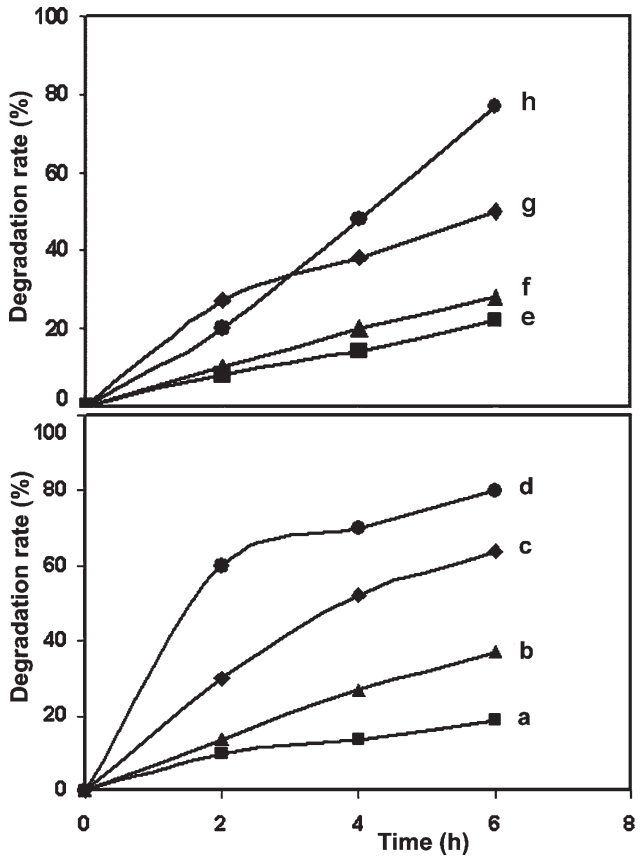

Figure 10 Photocatalytic decomposition rate of MB and EY versus irradiation time. (a) MB on untreated PAN fiber, (b) EY on untreated PAN fiber, (c) EY on ZnO-coated PAN fiber, (d) MB on ZnO-coated PAN fiber, (e) MB on untreated wool fiber, (f) EY on untreated wool fiber, and (g) EY on ZnO-coated wool fiber, (h) MB on ZnO-coated wool fiber.

The photocatalytic activity of the ZnO-coated fabrics is attributed to the dispersed ZnO nanoparticles with satisfactory crystallinized on the fibers surface. It has been established that the photocatalysed degradation of organic matters is initiated by photoexcitation of the semiconductor with energy greater than its band gap energy, followed by the formation of an electron-hole pair on the surface of catalyst [eq. (1)]. The high oxidative potential of the hole (h^+_{VB}) in the catalyst permits the direct oxidation of organic matter (dye) to reactive intermediates [eq. (2)]. Very reactive hydroxyl radicals can also be formed either by the decomposition of water molecules adhering to the surface of the photocatalyst [eq. (3)] or by the reaction of the hole with OH^- [eq. (4)]. The presence of water on samples surface were indicated by TGA analysis (Figs. 7 and 8). The hydroxyl radical is an extremely strong, nonselective oxidant ($E_0 = +3.06$ V) which leads to the partial or complete mineralization of several organic chemicals.[37–40]

$$ZnO + h\nu \rightarrow \mathrm{ZnO}(e^-_{CB} + h^+_{VB}) \quad (1)$$

$$h^+_{VB} + \mathrm{dye} \rightarrow \mathrm{dye}^{\bullet +} \rightarrow \text{oxidation of the dye} \quad (2)$$

$$h^+_{VB} + H_2O \rightarrow H^+ + {}^{\bullet}OH \quad (3)$$

$$h^+_{VB} + OH^- \rightarrow {}^{\bullet}OH \quad (4)$$

Electron in the conduction bond (e^-_{CB}) on the catalyst surface can reduce molecular oxygen to superoxide anion [eq. (5)]. This radical, in the presence of organic scavengers, may form organic peroxides [eq. (6)]) or hydrogen peroxide [eq. (7)].

$$e^-_{CB} + O_2 \rightarrow {}^{\bullet}O_2^- \quad (5)$$

$${}^{\bullet}O_2^- + \mathrm{dye} \rightarrow \mathrm{dye} - OO^{\bullet} \quad (6)$$

$${}^{\bullet}O_2^- + HO_2^{\bullet} + H^+ \rightarrow H_2O_2 + O_2 \quad (7)$$

Electrons in the conduction bond are also responsible for the production of hydroxyl radicals, species which have been indicated as the primary cause of organic matter mineralization [eq. (8)]. Therefore, the objective for cleaning and sterilization can be achieved by the assistance of a photocatalyst.

$${}^{\bullet}OH + \mathrm{dye} \rightarrow \text{degradation of the dye} \quad (8)$$

It is evident that ZnO-covered fibers promote the photodegradation process and the high surface area

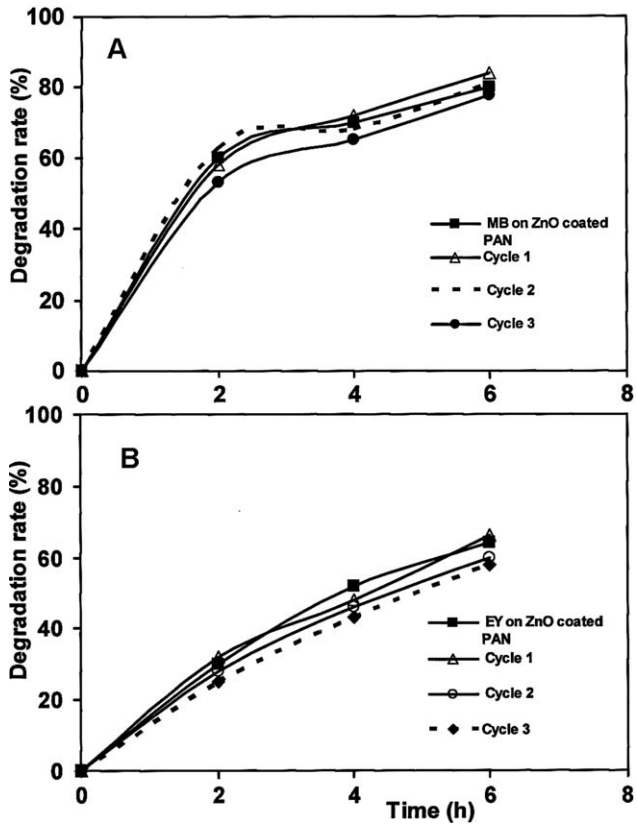

Figure 11 Photocatalytic efficiency of ZnO-modified PAN fiber upon repeated MB and EY adsorption-illumination cycles. A: MB adsorption-illumination cycles and (B) EY adsorption-illumination cycle.

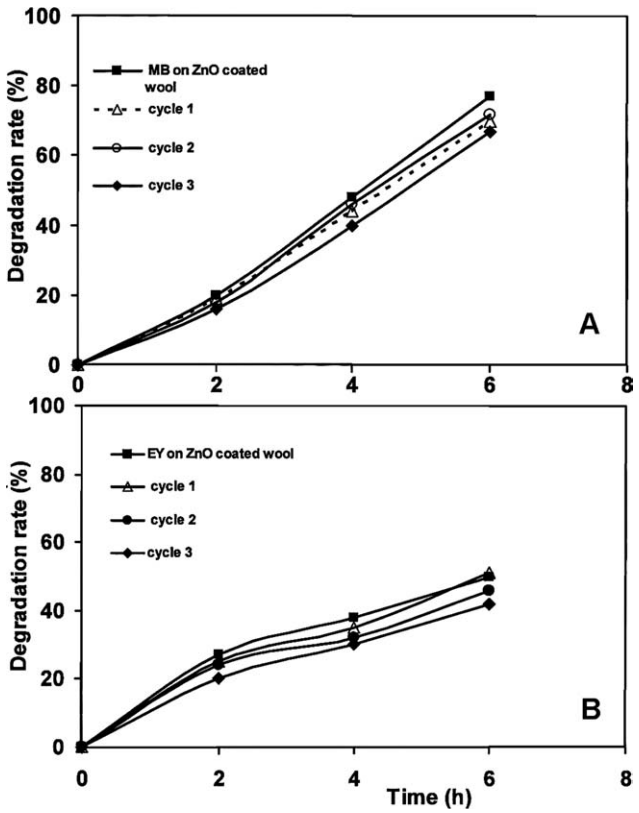

Figure 12 Photocatalytic efficiency of ZnO-modified wool fiber upon repeated MB and EY adsorption-illumination cycle. A: MB adsorption-illumination cycles and (B) EY adsorption-illumination cycle.

associated with the small particle size ensures a favorable condition.

Reuse of the ZnO-coated fibers

To test the durability of photocatalytic activity of the ZnO-coated fibers, the photodegradation process was repeated for three more cycles on the same sample. Figures 11 and 12 show the photocatalytic efficiency of the ZnO-modified fiber for the degradation of MB and EY, upon repeating cycles. There is a reduction of about 12 and 17% for photodegradation of MB and EY in ZnO-coated PAN fiber and also reduction of about 20 and 26% for degradation of MB and EY in case of ZnO-coated wool in photocatalytic activity following third cycle of reusing.

CONCLUSIONS

Nano-ZnO photocatalyst having wurtzite crystalline phase with high surface area were successfully prepared onto PAN and wool fiber via sol gel process at low temperature. Nanosized ZnO-covered fibers possess significant photocatalytic self-cleaning properties. They show high photocatalytic efficiencies in decomposing the preadsorbed MB and EY under UV-vis light. The dye degradation method was used to evaluate the photocatalytic activity of self-cleaning materials via a diffuse reflectance spectroscopic technique. The photoactivity of ZnO-coated fibers is attributed to the dispersed ZnO nanoparticles which are satisfactory crystallized on the fabric surface. The reusability of the ZnO-coated fibers are maintained upon several photodegradation cycles. Supported ZnO particles on PAN and wool substrate promote the photodegradation process and the high surface area associated with the small particle size ensures a favorable condition for self-cleaning purposes. This innovation is important because it should allow its practical use for industrial applications.

References

1. Sun, J. H.; Dong, S.Y.; Wang, Y. K.; Sun, S. P. J Hazard Mater 2009, 172, 1520.
2. Anandan, S.; Vinu, A.; Mori, T.; Gokulakrishnan, N.; Srinivasu, P.; Murugesan, V.; Ariga, K. Catal Commun 2007, 8, 1377.
3. Yassıtepe, E.; Yatmaz, H. C.; Oztürk, C.; Oztürk, K.; Duran, C. J Photochem Photobiol A 2008, 198, 1.
4. Yu, J. G.; Yu, X. X. Environ Sci Technol 2008, 42, 4902.
5. Height, M. J.; Pratsinis, S. E.; Mekasuwandumrong, O.; Praserthdam, P. Appl Catal B 2006, 63, 305.
6. Shen, W.; Li, Z.; Wang, H.; Liu, Y.; Guoa, Q.; Zhang, Y. J Hazard Mater 2008, 152, 172.
7. Guan, H.; Zhu, L.; Zhou, H.; Tang, H. Anal Chem Acta 2008, 608, 73.
8. Allain, E.; Besson, S.; Durand, C.; Moreau, M.; Gacoin, T.; Boilot, J. P. Adv Funct Mater 2007, 17, 549.
9. Tung, W. S.; Daoud, W. A. Acta Biomaterialia 2009, 5, 50.
10. Guan, K. Surf Coat Technol 2005, 191, 155.
11. Liu, Z.; Zhang, X.; Murakami, T.; Fujishima, A. Sol Energy Mater Sol Cells 2008, 92, 1434.
12. Wu, D.; Long, M.; Zhou, J.; Cai, W.; Zhu, X.; Chen, C.; Wu, Y. Surf Coat Technol 2009, 203, 3728.
13. Yaghoubi, H.; Taghavinia, N.; Alamdari, E. K. Surf Coat Technol 2010, 204, 1562.
14. Mejía, M. I.; Marín, J. M.; Restrepo, G.; Pulgarín, C.; Mielczarski, E.; Mielczarski, J.; Arroyo, Y.; Lavanchy, J.-C.; Kiwi, J. Appl Catal B 2009, 91, 481.
15. Mellott, N. P.; Durucan, C.; Pantano, C. G.; Guglielmi, M. Thin Solid Films 2006, 502, 112.
16. Kong, J. Z.; Li, A. D.; Zhai, H. F.; Gong, Y. P.; Li, H.; Wu, D. J Solid State Chem 2009, 2061, 182.
17. Lin, J. M.; Zhang, Y. Z.; Ye, Z. Z.; Gu, X. Q.; Pan, X. H.; Yang, Y. F.; Lu, J. G.; He, H. P.; Zhao, B. H. Appl Surf Sci 2009, 255, 6460.
18. Ko, H.; Tai, W.-P.; Kim, K.-C.; Kim, S.-H.; Suh, S.-J.; Kim, Y.-S. J Cryst Growth 2005, 277, 352.
19. Lee, J. B.; Kwak, S. H.; Kim, H. J. Thin Solid Films 2003, 423, 262.
20. Tan, S. T.; Chen, B. J.; Sun, X. W.; Hu, X.; Zhang, X. H.; Chua, S. J. J Cryst Growth 2005, 281, 571.
21. Lee, J.; Ko, K.; Park, B. J Cryst Growth 2003, 247, 119.
22. Wang, M.; Wang, J.; Chen, W.; Cui, Y.; Wang, L. Mater Chem Phys 2006, 97, 219.
23. Raoufi, D.; Raoufi, T. Appl Surf Sci 2009, 255, 5812.
24. Kim, K. T.; Kim, G. H.; Woo, J. C.; Kim, C. Surf Coat Technol 2008, 202, 5650.

25. Mao, Z.; Shi, Q.; Zhang, L.; Cao, H. Thin Solid Films 2009, 517, 2681.
26. Li, Q.; Chen, S.; Jiang, W. J Appl Polym Sci 2007, 103, 412.
27. Xu, B.; Caia, Z.; Wang, W.; Ge, F. Surf Coat Technol 2010, 204, 1556.
28. Chae, D. W.; Kim, B. C. J Appl Polym Sci 2006, 99, 1854.
29. Moafi, H. F.; Shojaie, A. F.; Zanjanchi, M. A. J Appl Polym Sci 2010, 2062, 118.
30. Yi, S. H.; Choi, S. K.; Jang, J. M.; Kim, J. A.; Jung, W. G. J Colloid Interface Sci 2007, 313, 705.
31. Sanchez-Soto, P. J.; Aviles, M. A.; del Rio, J. C.; Gines, J. M.; Pascual, J.; Perez-Rodriguez, J. L. J Anal Appl Pyrol 2001, 155, 58.
32. Wu, X.; Qin, W.; Ding, X.; Wen, Y.; Liu, H.; Jiang, Z. J Phys Chem Solids 2007, 68, 2387.
33. Yew, S.; Tang, H.; Sudesh, K. Polym Degrad Stab 2006, 91, 1800.
34. Mills, A.; Lepre, A.; Elliott, N.; Bhopal, S.; Parkin, I.; O'Neill, S. A. J Photochem Photobiol A 2003, 160, 213.
35. Mills, A.; Wang, J. J Photochem Photobiol A 2006, 182, 181.
36. Zhao, J.; Xu, L.; Yu, J.; Lv, Z.; Yuan, Q. Chin. Pat. CN 1,603,786A (2005).
37. Chakrabarti, S.; Dutta, B. K. J Hazard Mater 2004, 112, 269.
38. Hsiao, K. C.; Liao, S. C.; Chen, Y. J Mater Sci Eng A 2007, 447, 71.
39. Galindo, C.; Jacques, P.; Kalt, A. J Photochem Photobiol A 2000, 130, 35.
40. Daneshvar, N.; Salari, D.; Khataee, A. R. J Photochem Photobiol A 2004, 162, 317.